The Effects of Package Parasitics on the Stability of Microwave Negative Resistance Devices

JOHN W. MONROE

Abstract—The results of investigations of the effect of parasitic package elements on the behavior of negative resistance amplifiers are presented. Three different package styles were considered. Also two different lead configurations were used. The packages were all mounted in 7-mm coaxial transmission line.

The impedance of packages with and without leads was measured from 4 to 18 GHz using a manual network analyzer. These data were used as the basis for calculations to determine the values of elements in a simple three-element equivalent circuit model of the package.

Using the equivalent circuit model experimentally derived for each package style, the impedance seen by the chip through the package to a 50-Ω load was calculated. Broad-band curves of the impedance seen by the chip are presented. The experimentally derived model of the package permits matching of chip and package for stability.

TRANSFERRED electron (TE) and IMPATT devices operated as amplifiers are now being considered as possible replacements for traveling-wave tubes in applications where moderate power output, reasonable noise performance, and solid-state reliability are needed. Stability, or freedom from oscillation, is often important to the system designer. Stable active devices are important to the amplifier builder as well, because the impedance of a stable device can be measured directly. Knowledge of the device impedance facilitates accurate circuit design.

Establishing experimentally the proper conditions for stability is difficult, given the broad-band negative resistance characteristics of TE or IMPATT devices. An important factor affecting the stability of the negative resistance device is the microwave impedance of the package in which the device is mounted. The purpose of this paper is to help the amplifier designer choose a device package which provides the RF conditions for stable operation.

The paper consists of two main parts. First, the effects of the RF circuit, and especially the package, on negative resistance chip stability are discussed. Experimental data on a variety of package styles and lead configurations were accumulated during the course of this work. These data are used to provide a picture of the broad-band impedance seen by the active chip at its terminals. The broad-band impedances seen by the chip determine the suitability of certain package styles for use over specific frequency ranges.

The second part of the paper presents the results of experimental attempts to stabilize TE devices based on the information obtained in the study of package characteristics.

Experimental Setup

The Ceramics International A921, A251, and Minipak package styles were experimentally evaluated. Each package consists of a cylinder of ceramic material brazed to a gold-

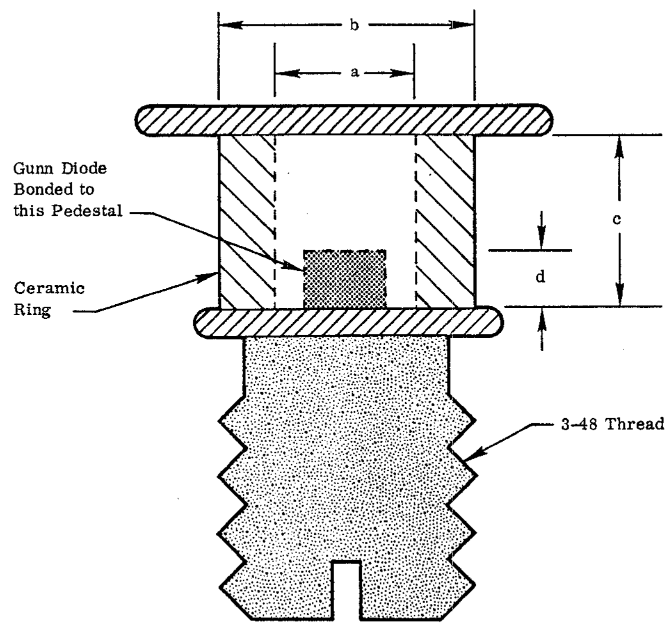

Fig. 1. General outline of ceramic-metal package.

plated copper pin as shown in Fig. 1. The active device is normally bonded to the head of the gold pin, and a lead is bonded from the top of the chip to the gold-plated Kovar ring brazed to the top of the ceramic cylinder. Two different lead configurations were used in the experiments described here: a single 1.5-mil-diameter gold wire; and two 10-mil-wide mesh straps crossing at the chip. A gold-plated Kovar cap, welded to the Kovar ring, completes the package. The dimensions identified by letters in Fig. 1 are presented in Table I for each package style.

The package impedance measurements and the TE device stability measurements were made in 7-mm coaxial 50-Ω transmission line. A manual network analyzer was used to make the impedance measurements. Details of the package mounting arrangement are given in Fig. 2. The reference plane for all measurements was established at the plane where the center conductor of the coaxial line joined the top hat of the package.

Modeling of the Package

A simple model accurately describes the impedance of the package and its coaxial mount over a broad frequency range, in some cases to 18 GHz. The model, consisting of two inductors and a capacitor arranged in a tee network, is shown in Fig. 3. The capacitor C_p is associated with the capacitance of the ceramic cylinder and the parasitic capacitances of the mounting configuration. The inductor L_l can be thought of as the inductance of the lead. The inductance L_p is associated with the transition from the mounting block to the coaxial

Manuscript received February 2, 1973; revised April 4, 1973. This work was supported by the Watkins-Johnson Company.

The author was with the Watkins-Johnson Company, Palo Alto, Calif. 94304. He is now with Hewlett-Packard, Palo Alto, Calif. 94304.

TABLE I

Package Style	Dimension "a" (mils)	Dimension "b" (mils)	Dimension "c" (mils)	Dimension "d" (mils)
A921	50	80	33	12
Pill-Prong (A251)	50	80	66	41
Minipak	15	33	12	3

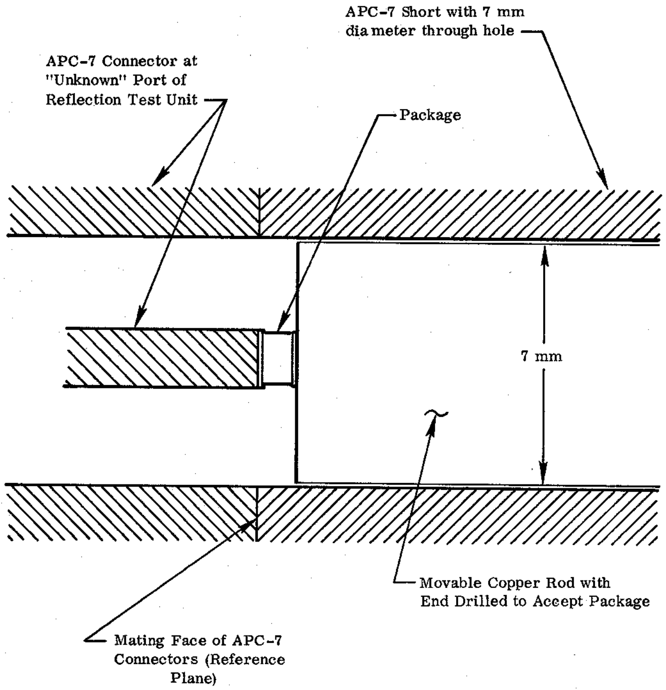

Fig. 2. Detail of package mounting arrangement.

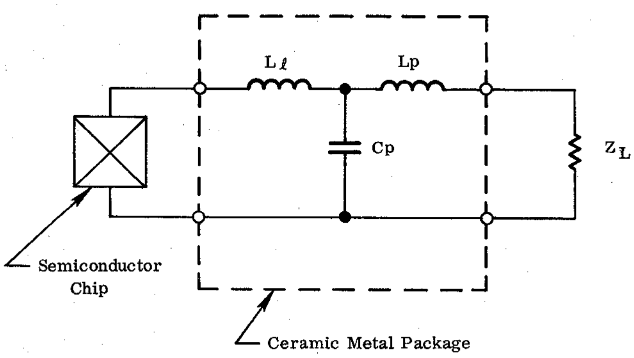

Fig. 3. Equivalent circuit of ceramic-metal package in mount of Fig. 2.

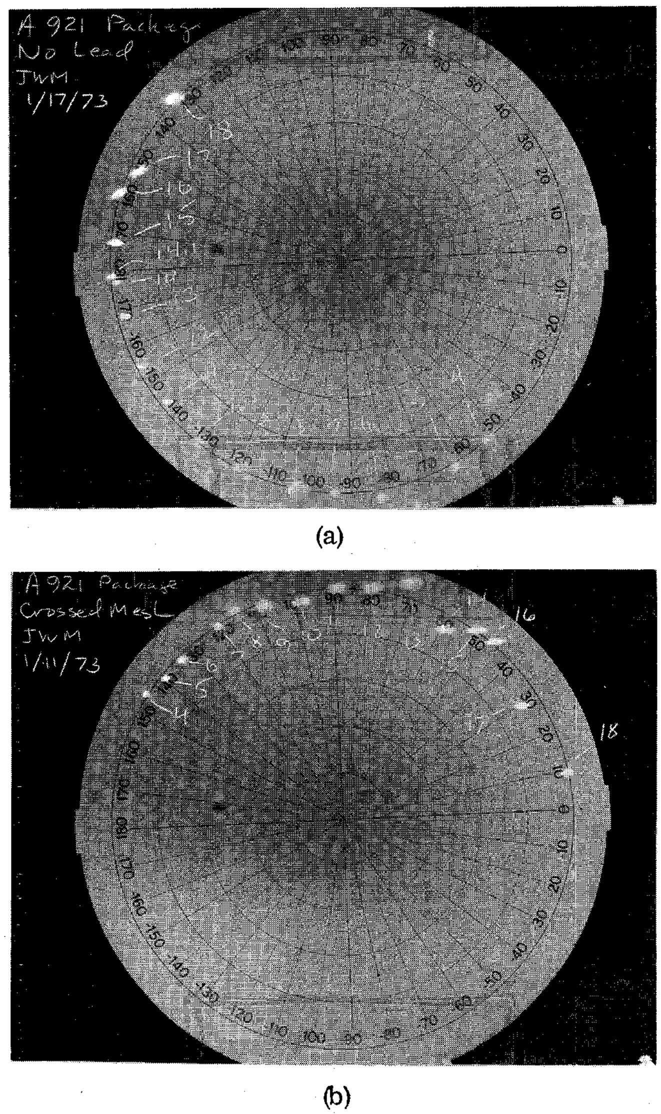

Fig. 4. Measured values of A921 package impedance. (a) With no lead. (b) With crossed mesh lead.

line. Other models of package parasitics have been derived [1], [2], [6]. Also different or more complex models may be needed to provide an accurate broad-band equivalent circuit for the package in mounts such as waveguide or microstrip. However, the model of Fig. 3 worked well for the experiments described in this paper and was consistent with the physical characteristics of the package and the coaxial mount.

To determine the individual elements of the package model, several packages of each style were prepared without active chips. For each package style, packages with and without leads were measured. In the packages with leads the leads were bonded from the metal ring on the ceramic to the gold-plated copper pedestal.

The impedances of packages with and without leads were measured in 1-GHz intervals from 4 to 18 GHz. At each frequency the reference plane was carefully established with an APC-7 coaxial short circuit. Resonant frequencies were measured as accurately as possible with a manual network analyzer, to within at least ± 1 percent. Typical data for the A921 package (Ceramics International) without a lead and with crossed mesh are shown in Fig. 4.

Measurements of packages without leads gave the data

TABLE II

SUMMARY OF PACKAGE PARASITIC ELEMENT VALUES

Package Style	Lead Configuration	Lp(nh)	Cp(pf)	Lℓ(nh)	f max.
A921	Crossed Mesh	0.36	0.35	0.22	18
A921	1.5 mil Diameter Wire	0.36	0.35	0.82	13
Pill-Prong (A251)	Crossed Mesh	0.48	0.25	0.40	18
Pill-Prong (A251)	1.5 mil Diameter Wire	0.48	0.25	1.04	10
Minipak	Crossed Mesh	0.20	0.32	0.09	18
Minipak	1.5 mil Diameter Wire	0.20	0.32	0.24	18

necessary to permit calculation of L_p and C_p. The package capacitance C_p is related to the measured open circuit package impedance X_c, the frequency f, and the resonant frequency f_r by the following expression:

$$C_p = \frac{1}{2\pi X_c}\left(\frac{f^2 - f_r^2}{f f_r^2}\right). \tag{1}$$

A final value of C_p is determined by averaging the values of C_p obtained from (1) at each measuring frequency. The values of C_p at each measuring frequency varied no more than ± 10 percent from the average, in the worst case.

The inductance L_p is simply

$$L_p = \frac{1}{(2\pi f_r)^2 C_p}\,. \tag{2}$$

Once L_p and C_p are known, L_l can be calculated from measurements of the package with a lead. The inductance L_l is related to L_p, C_p, the measuring frequency f, and the measured impedance X_p by the expression:

$$L_l = \frac{2\pi f L_p - X_p}{(2\pi f)^3 L_p C_p - 2\pi f - (2\pi f)^2 C_p X_p}\,. \tag{3}$$

As with C_p, the final value of L_l is determined by averaging the values of L_l calculated for each frequency.

Using the experimental values of package impedance and frequency in (1)–(3), L_l, L_p, and C_p were calculated for each package style. These values appear in Table II. The limit frequency for accuracy of each model is also given in the table. In the cases of the A921 and A251 packages with 1.5-mil-diameter gold wire leads, the limit frequency is the frequency at which the value of L_l calculated from (3) dropped to less than 10 percent of the average value. For the other package and lead configurations, the limit frequency is set by the upper operating frequency limit of the network analyzer used to make the impedance measurements.

The values of L_l, L_p, and C_p given in Table II are average values obtained from measurements of at least five packages with a given lead configuration. Parasitic element values did not vary more than ± 5 percent from package to package.

EFFECTS OF PACKAGE ON STABILITY

A negative resistance device such as the TE device will be stable if either or both of the following conditions on device impedance Z_d and circuit impedance Z_c are satisfied over the frequency range for which the device shows negative resistance:

$$\mathrm{Re}\,(Z_d) + \mathrm{Re}\,(Z_c) > 0 \tag{4}$$

$$\mathrm{Im}\,(Z_d) + \mathrm{Im}\,(Z_c) \neq 0. \tag{5}$$

Design of a circuit to satisfy conditions (4) and (5) requires knowledge of the active device impedance and the impedance of the RF circuit, preferably over the frequency range for which the device resistance is negative. The package equivalent circuit data presented in Table II allows the circuit designer to calculate the actual load seen by the chip through the package. As an example, the element values in Table II were used to calculate the RF impedance seen by the semiconductor chip looking through the package to a 50-Ω load. This is the same impedance seen by the chip when it is packaged and mounted as shown in Fig. 2. The impedances for different package styles are plotted in Figs. 5–7 as functions of frequency up to the limit frequency.

The data of Figs. 5–7 can be used to avoid packages which might permit the active device to oscillate in a coaxial 50 circuit A TE device, for example, has an equivalent circuit consisting of a frequency dependent resistor in series with a frequency dependent capacitor [3]. The TE device exhibits negative resistance over an octave or more. Assuming a TE device with negative resistance from 8 to 16 GHz, it is obvious from Figs. 5–7 that either the A921 or Minipak style packages with crossed mesh leads are most likely to prevent oscillation. Both packages transform the 50-Ω load to a positive resistance and capacitive reactance over the full 8–16-GHz frequency range. Condition (5) is satisfied, and the device cannot oscillate.

In most circulator-coupled reflection amplifiers, a lossless equalizer network is placed between the packaged active chip and a 50-Ω circulator [6]. Plots of impedance at the chip terminals versus frequency similar to Figs. 5–7 can be obtained by transforming the 50-Ω circulator impedance first through the equalizer network and then through the package equivalent network. Such plots, coupled with knowledge of the impedance of the active chip, can be used to insure freedom from oscillation in reflection amplifier design

EXPERIMENTAL RESULTS

To test the idea that choice of a package could make similar chips either stable or unstable, chips from a single wafer were bonded into two packages, the A921 with crossed mesh and the A251 package with 1.5-mil-diameter wire lead. The doping level of the active layer was nominally 1.3×10^{15} cm^{-3} and the layer thickness was 8 μm. These chips when stabilized displayed negative resistance from roughly 9 to more than 18 GHz, as shown in Fig. 8.

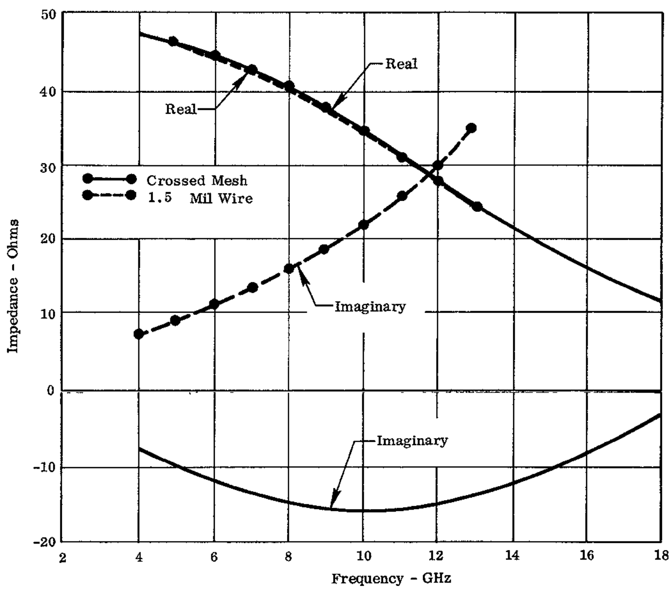

Fig. 5. Impedance seen by chip of a 50-Ω load transformed through the A921 package for two lead configurations.

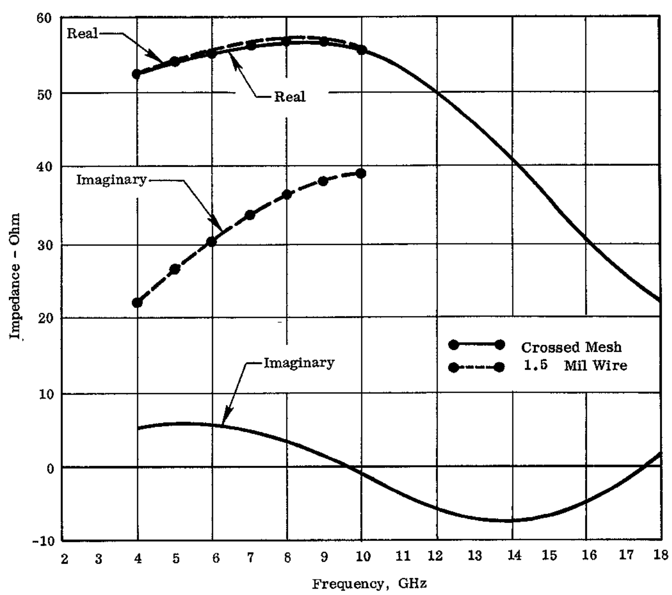

Fig. 6. Impedance seen by chip of a 50-Ω load transformed through the A251 package for two lead configurations.

The packaged devices were placed in the circuit of Fig. 2. In the A921 package the chips operated stably at voltages from slightly above the 3-V threshold to 15 V. In the A251 package, the devices oscillated between 12 and 16 GHz, regardless of bias voltage. These chips, bonded in A921 packages, were ultimately used in the 12-GHz 5-percent bandwidth amplifier shown in Fig. 9.

The detailed characteristics of the amplifier appear in Table III. In building this three-stage amplifier, 7-mm coaxial circuits were used. Gain level was set for each stage with a single low impedance section of transmission line in series with the packaged TE device. The frequency of the gain peak was determined by the length of the transmission-line section.

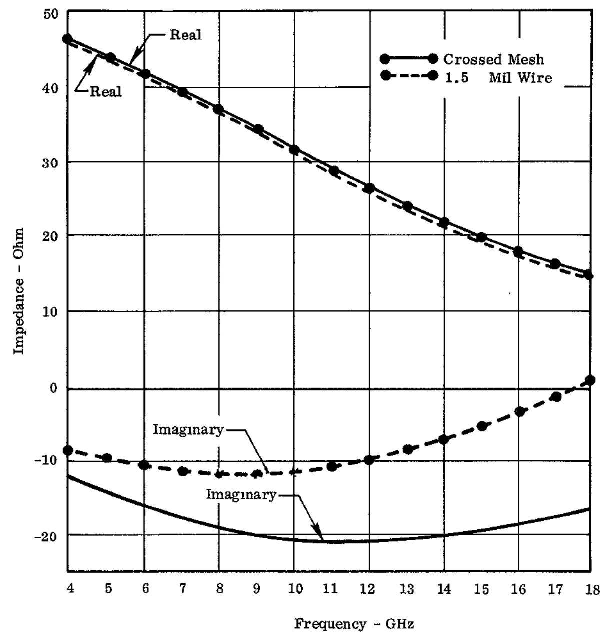

Fig. 7. Impedance seen by chip of a 50-Ω load transformed through the Minipak package for two lead configurations.

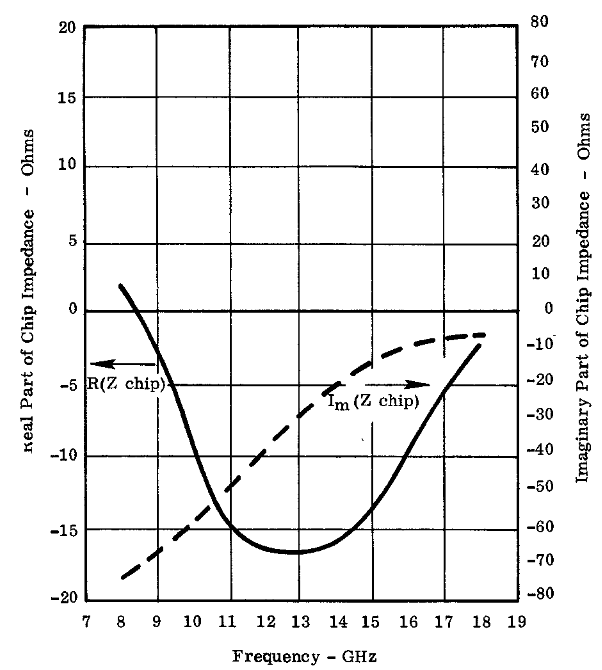

Fig. 8. Impedance of chip 305-15 operated at 12.5 V, approximately four times threshold. At twice threshold the chip resistance at 15 GHz is −40 Ω.

The impedance seen by the chip through the package and the length of transmission line was such that conditions (4) and (5) were satisfied over the full negative resistance passband of the TE device, thus insuring stability of the amplifier.

Correct choice of a package is not a foolproof method of stabilizing TE devices. The TE chip itself must be capable of stable operation. Indications are that contacts, doping profiles, length, and thickness must all be considered in obtaining

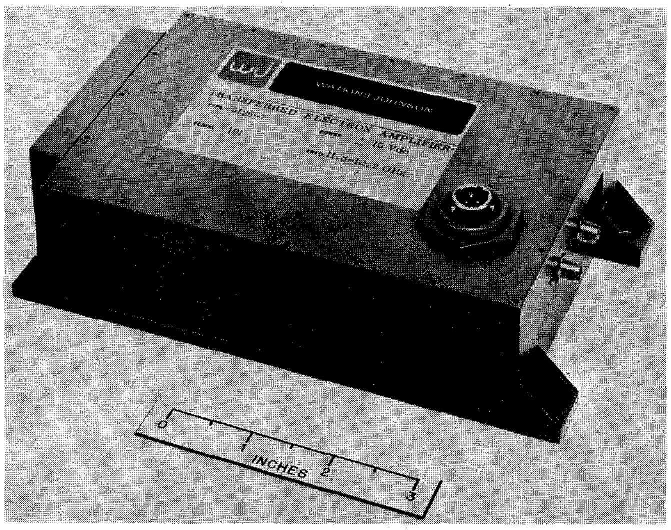

Fig. 9. Transferred electron amplifier.

stable operation [4], [5]. However, no supercritically doped chip will stabilize if operated in a poorly chosen package.

Conclusions

Careful choice of package and lead configurations is an important element of successful negative resistance amplifier design at frequencies above 8 GHz. The three package styles and two lead configurations discussed in this paper provide a sampling of the wide range of package parasitic element values which can be obtained. As was demonstrated in experiments with TE devices, correct choice of package configuration (and thus package parasitic element values) can insure stability of the active device. A sanguine choice of a package with the appropriate parasitic elements can also provide the first elements of a broad-band matching network.

The experiments and calculations reported here are applicable to 7-mm coaxial systems. The equivalent circuit elements listed in Table II include the parasitic elements of the coaxial mounting configuration. However, the techniques of determining the package and mount parasitic elements can be applied directly to other mounting configurations (e.g., stripline, shunt mounting in coaxial line, etc.).

The package parasitic element values listed in Table II are valid only over limited frequency ranges. More sophisticated models for the different package styles such as the model suggested by Owens and Cawsey [1] for the S-4 package will be accurate to higher frequencies than the model presented in Fig. 3 of this paper. However, the broad-band models presented in this paper for different package styles will ease the design of broad-band high-performance amplifiers between 4 and 18 GHz.

TABLE III

Performance Characteristics of the Amplifier of Fig. 9

Frequency Range:	11. 8 GHz to 12. 2 GHz
Gain:	25 dB
Gain Variation with Frequency:	± 0. 25 dB/85 MHz
Maximum Gain Slope:	± 0. 015 dB/MHz
Gain Variation with Temperature:	± 1 dB
1 dB Gain Compression Point:	+16 dBm
Input/Output VSWR:	1. 2:1 Maximum
Noise Figure:	23 dB
Spurious Output:	Less than -65 dBm
Temperature Range:	10°C to 50°C
Operating Voltage/Current:	15 volts, 1. 05 amperes
Weight:	2. 0 lbs.

Acknowledgment

The author would like to thank Dr. E. F. Johnson for his interest and technical suggestions during the course of this work, and Dr. W. K. Kennedy, Jr., for his support. He would also like to thank S. A. Kern for his help in taking the data, and Mrs. M. C. Wagner and Mrs. A. G. Hallin for their excellent work in fabricating the test packages and packaged TE devices.

References

[1] R. P. Owens and D. Cawsey, "Microwave equivalent-circuit parameters of Gunn-effect-device packages," *IEEE Trans. Microwave Theory Tech.* (*Special Issue on Microwave Circuit Aspects of Avalanche-Diode and Transferred Electron Devices*), vol. MTT-18, pp. 790–798, Nov. 1970.

[2] R. P. Owens, "Mount independent equivalent circuit of the S-4 diode package," *Electron Lett.*, vol. 7, pp. 580–582, Sept. 23, 1971.

[3] B. S. Perlman, C. L. Upadhyayula, and R. E. Marx, "Wide band reflection-type transferred electron amplifiers," *IEEE Trans. Microwave Theory Tech.* (*Special Issue on Microwave Circuit Aspects of Avalanche-Diode and Transferred Electron Devices*), vol. MTT-18, pp. 911–921, Nov. 1970.

[4] S. Y. Narayan and F. Sterzer, "Stabilization of transferred-electron amplifiers with large $\eta_0 l$ products," *Electron. Lett.*, vol. 5, pp. 30–31, Jan. 1969.

[5] P. Jeppesen and B. Jeppsson, "The influence of diffusion on the stability of the supercritical transferred electron amplifier," *Proc. IEEE* (Lett.), vol. 60, pp. 452–454, Apr. 1972.

[6] C. L. Upadhyayula and B. S. Perlman, "Design and performance of transferred electron amplifiers using distributed equalizer networks," *IEEE J. Solid-State Circuits*, vol. SC-8, pp. 29–36, Feb. 1973.